JTTEE5 19:1013–1023
DOI: 10.1007/s11666-010-9495-y
1059-9630/$19.00 © ASM International

Wear-Resistant Amorphous Iron-Based Flame-Sprayed Coatings

J. Voyer

(Submitted November 24, 2009; in revised form February 15, 2010)

The flame-spraying process (powder and wire) was used to spray Nanosteel SHS-7170 powder and Eutectic-Castolin EnDOtec DO-390N wire onto aluminum and mild steel substrates to produce partially amorphous iron-based coatings. The phase content and the wear resistance of the coatings were evaluated in the as-sprayed condition only. The results obtained showed that the powder and wire flame iron-based coatings performed relatively well in terms of wear resistance. The coating microstructure, phase content, hardness, and wear performance all depended strongly on the spraying parameters used. This study showed that amorphous iron-based coatings with good wear resistance could be produced using the flame-spray process, showing that this process appeared to be a suitable inexpensive alternative to plasma or high velocity oxygen-fuel spraying processes.

Keywords friction and wear, influence of spray parameters, nanostructured materials, quasicrystalline coating, super hard steel coatings

1. Introduction

The production of low-emission CO_2 automobiles is, since the Kyoto protocol, of ever-growing concern to the automotive industry, governments, and end-users. The implementation of new environmental regulations is forcing the industry to find solutions that will decrease emissions. One of these is to replace steel parts with specific aluminum alloy parts. Since aluminum is about 3 times lighter than steel, it has a direct influence on overall fuel consumption when it replaces steel parts in automobiles. However, aluminum alloys have a major drawback: their wear resistance is too low for them to be deployed in specific automobile areas where wear mechanisms are present. Applying wear-resistant coatings to aluminum alloy parts in the automotive industry could overcome this flaw.

Flame spraying represents an efficient alternative to plasma or high velocity oxygen-fuel spraying (HVOF) processes in producing coatings due to its lower gas consumption and the lower cost of its feedstock materials, especially for wires. The process is also extremely simple and requires low-cost equipment which may be portable for on-site applications. The flame-spray process (powder or wire) involves the continuous combustion of a fuel gas, and the hot gases are released through the nozzle cap. The powder or wire is fed axially and centrally into the flame and melts. The molten powder particles or wire droplets are then accelerated in the process gas stream and travel until they reach and impact on the surface to be coated, i.e., the substrate. On impact, the particles deform and cool down rapidly to form the coating.

Iron-based powders and wires, which via thermal spray processes can produce coatings with a mixture of amorphous and nanostructured microstructures, have been developed in the last few years, are nowadays commercially available, and have been previously investigated (Ref 1-4). These new materials, when used as wear and corrosion protection coatings, are believed to perform better than the conventional HVOF-sprayed WC-based coatings due to their ability to form a mixture of amorphous and nanostructured microstructures (Ref 4-10). In addition, the thermal conductivity of these coatings is comparable to or slightly higher than that of ceramics and can therefore also be used as thermal barrier coatings for low-temperature combustion engines (Ref 11).

This article aims to demonstrate that iron-based amorphous/nanostructured coatings produced using the flame-spray process for typical wear protection applications in the automotive or any other industry could be a cost-effective and efficient alternative to plasma or HVOF-sprayed wear-resistant coatings.

2. Materials and Experimental Procedure

The coatings were produced using either a Nanosteel SHS-7170 powder or a Eutectic-Castolin EnDOtec DO-390N wire. The water-atomized Nanosteel powder was iron-based (51%Fe-20%Cr-10%W-5%B-5%Mn-5%Mo-2%C-2%Si), had a spherical morphology, and a size distribution of −53+15 μm. The filled wire consisted of a powder (61%Fe-15%Cr-8%W-4%B-4%Nb-4%Mo-2%C-1%Mn-1%Si) contained in an iron-based shell and had an outside diameter of 1.6 mm.

J. Voyer, Leichtmetallkompetenzzentrum Ranshofen GmbH (LKR), Austrian Institute of Technology, Postfach 26, 5282 Ranshofen, Austria. Contact e-mail: joel.voyer@ait.ac.at.

Aluminum and mild steel samples with dimensions of 35 mm × 35 mm × 3 mm were used as substrates. Deploying mild steel substrates makes it possible to study the influence, if any, of the substrate material on the microstructure and the phase content of the sprayed coatings, and on their wear resistance.

The flame spraying of the coatings was performed using a Metco 5P-II powder flame-spray gun (Metco, Westbury, NY) and a GTV-12E wire flame-spray gun (GTV GmbH, Luckenbach, Germany). Prior to spraying, the aluminum and mild steel substrates were degreased and grit-blasted via standard procedures. Table 1 and 2 lists the spraying parameters used to produce the coatings with the powder or the wire spray gun.

The samples were sprayed using a typical meander movement of the spray gun, which was mounted on a 6-axis ABB robot while the samples were kept stationary. To cool the samples during the spraying process, two air amplifiers were directed toward the substrate surfaces. As shown in Table 1 and 2, the positions of these amplifiers were changed to observe the effect of the cooling on the coating properties: (i) the amplifiers were fixed in the spray booth in front of the substrates to be coated and did not move; or (ii) the amplifiers were mounted on the robot arm and moved along with it. For each parameter set, a total of eight samples were produced (4 on Al and 4 on mild steel substrates): two of each coated substrate type (Al and steel) were used in the as-sprayed condition, and two were kept for future heat treatments to evaluate the effect of heat treatments on coating properties. The influence of the heat treatments on the properties of the iron-based coatings (phase content, hardness, and wear resistance) will be part of a future study and are not presented here. One of the two as-sprayed samples was used for microstructural characterization and phase content identification, and the other was used to perform wear tests.

The resulting as-sprayed coatings were prepared and investigated by optical microscopy to obtain information concerning coating porosity and microstructure and the interface between the coating and the substrate. For each coating, four different porosity measurements were performed and the reported value is the average of these measurements.

The hardness of the coatings was evaluated using a microhardness tester (LECO model LM700AT) with a 300 g load applied for 15 s, and the reported value is an average of five different measurements, which were performed on different cross-section locations of the sprayed coatings. The hardness measurements were performed in the half-thickness near the surface of the coatings to better correlate these hardness values with the wear tests results, which represent the coatings surface wear resistance. Furthermore, the size of the hardness indentations was big enough to cover several different phases of the coatings and thus the reported hardness values represent the overall coating hardness.

The phase content was identified using a commercial X-ray diffractometer (X'Pert Pro, PANanalytical) with a Cu-K_α radiation at a voltage and current settings of 38 kV and 45 mA, respectively, for 2θ angles between 35° and 85° using a scan rate of 0.3°/min. The resulting peaks were identified by comparing them with standardized JCPDS data files.

The wear performance of the different as-sprayed coatings was tested using a commercially available ball-on-disk tribometer (Model TRN, CSM Instruments, Peseux, Switzerland). The Al_2O_3 ball had a diameter of 6 mm and the applied load between the ball and the coating surface was 8 N. The relative linear velocity was 25 cm/s, and the total test length was 2000 m. The tests were performed at room temperature and under dry sliding conditions. These conditions do not fully correspond to the conditions generally encountered in engines,

Table 1 Powder flame-spray parameters used for producing amorphous/nanostructured iron-based coatings

Sample	C_2H_2, L/h	O_2, L/h	Total gas flow, L/h	O_2/C_2H_2	Standoff distance, mm	Powder feed rate, g/min	Cooling air position	Substrate temperature, °C	# of layers
P1	880	1415	2292	1.6	65	80	Fixed	150	5
P2	880	1415	2292	1.6	65	80	On robot arm	150	5
P3	1100	1080	2668	1.6	65	80	Fixed	150	5
P4	1165	1835	3000	1.6	65	80	Fixed	165	5

Table 2 Wire flame-spray parameters used for producing amorphous/nanostructured iron-based coatings

Sample	C_2H_2, L/h	O_2, L/h	Total gas flow, L/h	O_2/C_2H_2	Standoff distance, mm	Wire feed rate, cm/min	Cooling air position	Substrate temperature, °C	# of layers
W1	880	1415	2292	1.6	65	100	On robot arm	120	35
W2	725	1550	2292	2.0	65	100	On robot arm	120	35
W3	1135	1140	2292	1.0	65	100	On robot arm	125	35
W4	1165	1835	3000	1.6	65	100	On robot arm	130	35

but nevertheless, they were used as a screening test. The width and depth of the sample wear scar cross-section was measured using a linear profilometer (SURTRONIC 25, Taylor-Hobson, Leicester, UK) and the corresponding wear cross-section area was calculated using the software provided with the profilometer (TalyProfile Silver, Taylor-Hobson, Leicester, UK). For each tested sample, four different measurements of the wear scar cross-section were performed, each at right angles to the other, to obtain an average value of the sample wear scar cross-section area.

The wear volumes of the coatings were then calculated using the following equation:

$$V_C = 2\pi R \times A_A, \quad \text{(Eq 1)}$$

where V_C is the coating wear volume (mm^3), R is the wear radius (4 mm), and A_A is the area of the wear scar cross-section (mm^2).

The averaged total coating wear rate (mm^3/N m) was calculated from the average coating wear volume (Eq 1) by using the following equation:

$$WR_C = \frac{V_C}{L \times l}, \quad \text{(Eq 2)}$$

where WR_C is the coating wear rate (mm^3/N m), V_C is the coating wear volume (mm^3), L is the load (8 N), and l is the test length (2000 m).

3. Results and Discussion

3.1 Coating Microstructure

As mentioned earlier, iron-based coatings were produced using the spraying parameters listed in Table 1 and 2 by means of the powder and wire flame-spray processes, respectively. Figure 1 and 2 shows typical microstructures of the different coatings produced using the powder or the wire feedstock materials. Depending on the spraying parameters used, the coatings are relatively porous or dense with porosity values ranging between 2.5 and 7.1% for powder-sprayed coatings and between 2.2 and 9.8% for wire-sprayed coatings, as reported in Table 3 and 4, which are approximately identical or slightly higher than similar coatings produced using HVOF (3 to 4%) (Ref 2), plasma (3 to 5%, ~15%) (Ref 5, 11), or wire arc (4 to 9%) processes (Ref 5). The microstructure of all coatings is relatively good with the presence of only few microcracks. For all the materials, the substrate-coating interfaces are excellent with no signs of defects such as cracks or embedded sand-blast particles. However, it was observed that for some of the samples, the coating partially spalled off at the edges of the substrates. This partial spallation often occurs at sharp edges of sprayed substrates or parts and is due to the increased stress encountered at these locations; this phenomenon is well known in the thermal spray community. However, in this study, the spallations were locally limited to a few millimeters from the substrate edges and therefore had no influence on the overall wear performance of the sprayed coatings.

3.2 Hardness

The measured hardness values and their standard deviations are reported in Table 3 and 4 for the powder and wire as-sprayed coatings on Al and steel substrates, respectively. The hardness values range between approximately 625 and 970 $HV_{0.3}$ depending on the spray parameters used. This hardness range is, as expected, slightly lower than previously reported hardness values for coatings produced using the HVOF spray process (1000 to 1100 $HV_{0.3}$) (Ref 4), but is surprisingly similar to those reported for coatings produced using plasma (600 to 800 $HV_{0.2}$) or wire arc (720 to 1030 $HV_{0.2}$) processes (Ref 5). The highest measured hardness values for the powder- and wire-sprayed coatings were determined for the P3 coatings on both aluminum and steel substrates and for the W2 and W3 coatings, also on both aluminum and steel substrates. On the other hand, the lowest measured hardness values were determined for both the coatings W1 and W2 on aluminum substrates, both with the highest porosity values. The high standard deviations reported for the hardness values are believed to be due to the inhomogeneous character of the coating microstructures. These results show that the production of flame-sprayed amorphous iron-based coatings with hardness values comparable to coatings produced using expensive thermal spray processes such as HVOF and plasma spraying can be achieved.

By looking in more detail at the hardness results for the powder-sprayed coatings on Al substrates presented in Table 3 and on steel substrates presented in Table 4, it is seen that the increase in the total gas flow rate from 2292 L/h (P1) to 2668 L/h (P3) to 3000 L/h (P4) presents a maximum hardness value (971 $HV_{0.3}$ for the Al substrates and 910 $HV_{0.3}$ for the steel substrates) obtained for the middle total gas flow rate of 2668 L/h (P3). The total gas flow rate has a direct influence on the particles' molten state and their velocities. Higher gas flow rates produce better molten and faster particles, both contributing to produce, as it is generally believed, harder coatings due to the higher deformation of the particles during their impact on the substrate. However, from the results presented here, it is observed that the highest flow rate used produced a coating having a lower hardness value than the coating produced with the middle flow rate. This may be due to a shorter residency time of the molten particles in the flame when the flow rate is higher, thus producing lesser molten particles and to the fact that such a high flow rate may produce splashing of the splats during their impact on the substrate, both enabling the possibility of a decreased hardness value. However, it is worth noting that the influences of such spray parameters on the coatings properties are quite complex and is not the main goal of this article.

As for the influence of the cooling location on hardness during the powder spraying of the coatings (cooling system fixed (P1) or placed on the robot arm (P2)), it is seen that when using Al substrates there is an increase when the cooling equipment moves with the robot. However, for the steel substrates, since the standard deviation of the

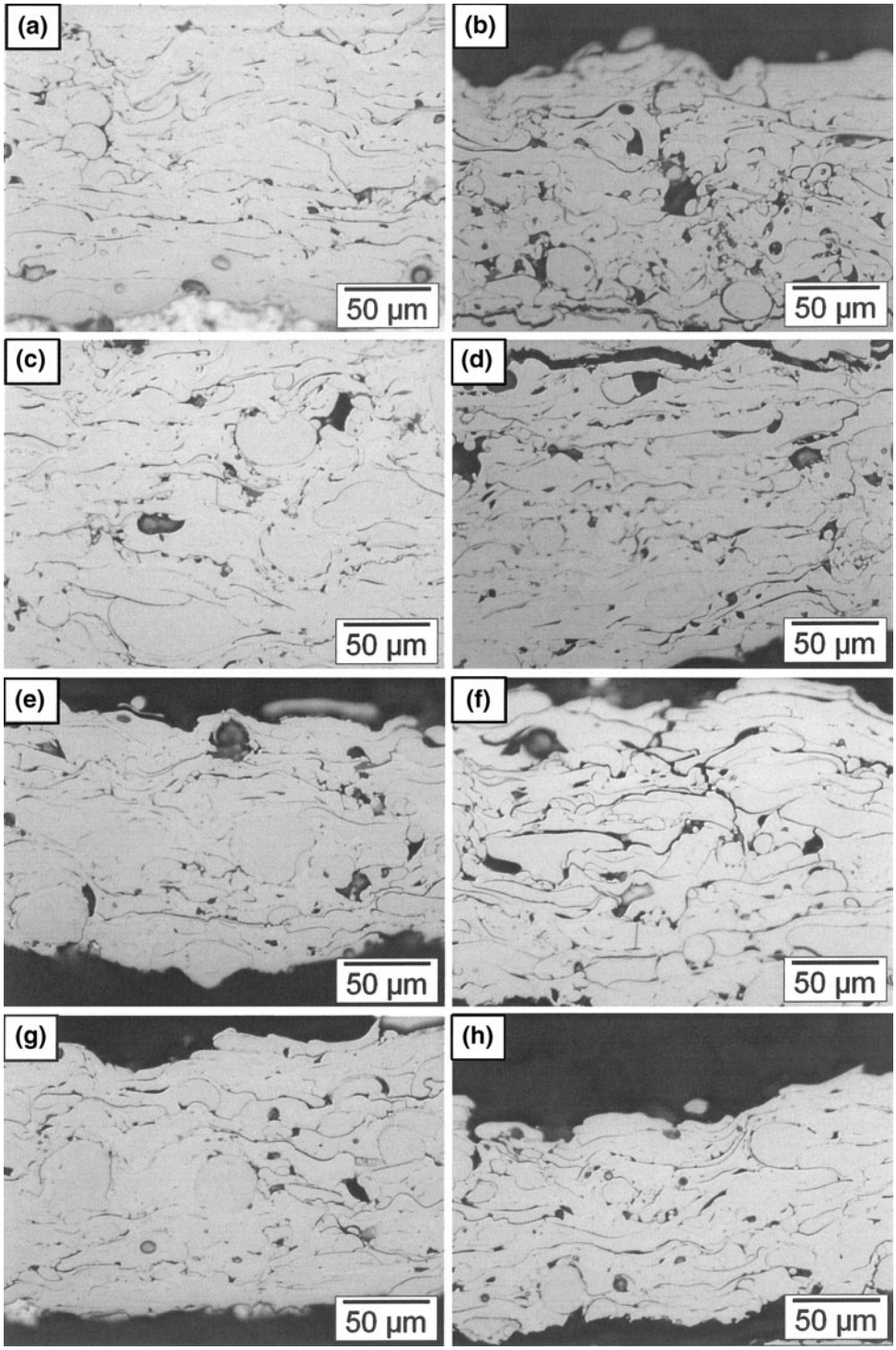

Fig. 1 Micrographs of the powder flame as-sprayed Fe-based coatings: (a) P1 on Al, (b) P1 on steel, (c) P2 on Al, (d) P2 on steel, (e) P3 on Al, (f) P3 on steel, (g) P4 on Al, and (h) P4 on steel

hardness for the coating P1 is extremely high, it is not possible to confirm whether there is a decrease or an increase in the hardness value when the cooling system is placed on the robot arm.

For the wire-sprayed coatings on Al substrates (Table 3) and on steel substrates (Table 4), the hardness value decreases from 820 $HV_{0.3}$ for the Al substrates and 889 $HV_{0.3}$ for the steel substrates to a value of 628 $HV_{0.3}$ for the Al substrates and 734 $HV_{0.3}$ for the steel substrates when the O_2/C_2H_2 ratio is increased from 1.0 (W3) to 1.6 (W1) and slightly increases again to 693 $HV_{0.3}$ for the Al substrates and 877 $HV_{0.3}$ for the steel substrates when the

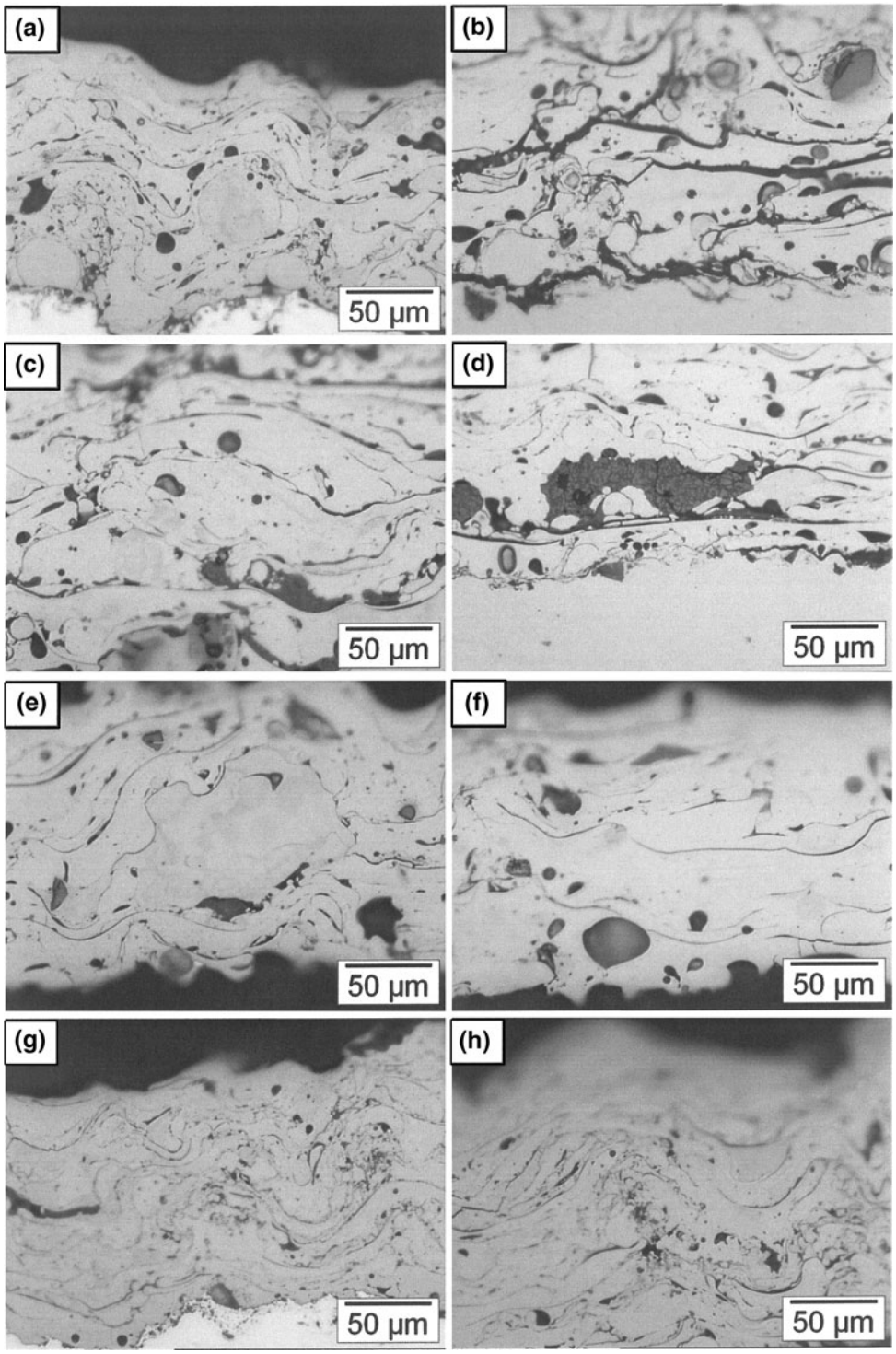

Fig. 2 Micrographs of the wire flame as-sprayed Fe-based coatings: (a) W1 on Al, (b) W1 on steel, (c) W2 on Al, (d) W2 on steel, (e) W3 on Al, (f) W3 on steel, (g) W4 on Al, and (h) W4 on steel

O_2/C_2H_2 ratio is increased further to 2.0 (W2). When the total gas flow rate is kept constant, the O_2/C_2H_2 ratio has a direct influence on the flame temperature and therefore on the particles molten and oxidation states. A ratio higher than the stoichiometry state (ratio = 1.6) means an excess of O_2. It would be then believed that a $O_2/C2_2H_2$ ratio of 2 would increased the oxidation state of the molten particles during the flame spray process and thus the presence of such a higher oxidation would produce harder coatings. However, this is not observed in the

Table 3 Properties of the amorphous/nanostructured iron-based as-sprayed coatings on Al substrates

Sample	Thickness, µm	Porosity, %	Hardness, $HV_{0.3}$	Crystallinity index
P1	295	3.3 ± 1.2	784 ± 32	0.97
P2	320	2.5 ± 1.4	912 ± 24	0.51
P3	240	2.5 ± 0.5	971 ± 93	0.15
P4	200	3.2 ± 1.3	784 ± 97	0.39
W1	335	9.8 ± 2.8	628 ± 52	0.22
W2	370	6.8 ± 2.4	693 ± 101	0.23
W3	455	2.2 ± 0.3	820 ± 113	0.97
W4	305	2.2 ± 1.2	765 ± 21	0.51

Table 4 Properties of the amorphous/nanostructured iron-based as-sprayed coatings on steel substrates

Sample	Thickness, µm	Porosity, %	Hardness, $HV_{0.3}$	Crystallinity index
P1	290	7.1 ± 2.8	826 ± 125	0.34
P2	325	4.4 ± 1.1	751 ± 94	0.66
P3	215	4.5 ± 1.5	910 ± 61	0.20
P4	205	4.3 ± 1.0	862 ± 100	0.48
W1	370	2.5 ± 0.7	734 ± 71	0.31
W2	420	4.7 ± 1.9	877 ± 82	0.24
W3	500	4.4 ± 0.3	889 ± 123	0.25
W4	415	4.4 ± 2.4	709 ± 65	0.45

results presented in this article: the highest hardness is found for the lower O_2/C_2H_2 ratio. Therefore, further investigations are needed to fully understand the influence of the spray parameters on the coatings properties, and as mentioned earlier, it is not the main goal of this article to fully describe these influences.

Regarding the influence of the total gas flow rate on the hardness during the wire spraying of the coatings, when using Al substrates there is a small increase in the hardness value when the flow rate goes up from 2292 L/h (W1) to 3000 L/h (W4). However, for the steel substrates, since the standard deviations in the hardness values for both coatings W1 and W4 are relatively high, it is difficult to confirm whether there is a small decrease or increase in the hardness value when the total flow rate is increased.

When looking at the influence of the substrates on the hardness of both powder- and wire-sprayed coatings, the different hardness values between the aluminum and steel substrates when using the same spray parameters are due to the different heat conductivity of both substrates and therefore to the heat transfer occurring between the molten particles upon their impact with the substrates. Since heat transfer has a significant influence on the coating formation and therefore on the coating microstructure and properties, the use of different substrate materials produces quite different coatings.

3.3 Phase Content

3.3.1 Powder-Sprayed Coatings. Figure 3 shows the XRD patterns of the powder-sprayed coatings on both aluminum and steel substrates. The XRD pattern of the starting powder is also shown for comparison purposes.

In the feedstock powder, FeCr, CrB, and CrFeB phases were found to be the major phases. In the as-sprayed coatings, the phases present depend strongly on the spray parameters used: for some coatings new peaks are observed in addition to those already found in the feedstock powder, and in other coatings, almost no peaks could be observed, indicating that amorphization may have taken place. The phases observed for the powder-sprayed coatings are similar to those reported elsewhere (Ref 5, 10, 11).

More precisely, for the coatings sprayed onto Al substrates, the samples P1, P2, and P4 show two new CrFeB peaks at an angle of 38.5° and 44° while maintaining part of the other main phases' starting powder peaks. The intensity of the new 38.5° peak was the strongest for sample P1 and about half for both samples P2 and P4, and the intensity of the new 44° peak was the strongest for samples P1 and P2 and very weak for sample P4. However, for sample P3 no new peaks were detected and only a weak peak (44.5°) was observed without any other peaks, which indicates that this coating may be mostly amorphous.

For coatings sprayed onto steel substrates, only sample P4 has a new CrFeB peak at an angle of 44° while maintaining part of the other main phases' peaks. However, for samples P1, P2, and P3 no new peaks were detected and either only a weak peak (44.5°) was observed with no other peaks (sample P3) or with other small peaks (sample P1), or a strong peak (44.5°) was observed combined with other small peaks (sample P2). This indicates that the P3 coating may again be predominantly amorphous. This may also apply to a lesser extent to sample P1.

When looking at the influence of the substrates on the phase content of the powder-sprayed coatings, the different phase contents of the coatings between the aluminum and steel substrates when using the same spray parameters are due, like for the hardness values presented previously, to the different heat conductivity of both substrates and therefore to the heat transfer occurring between the molten particles upon their impact with the substrates. Since heat transfer has a significant influence on the coating formation and phase content, the retention of the amorphous phase due to a very high cooling rate of the impinging molten spray particles is greatly influenced by the substrate material used.

The relative proportions of crystalline and amorphous phases present in the as-sprayed coatings were estimated by calculating the crystallinity index for all the powder-sprayed coatings on both substrate types (Al or steel). This index represents the ratio of the area of the crystalline phase peaks to the total area of the XRD spectrum. Table 3 lists the crystallinity index for the coatings sprayed on Al substrates and Table 4 the coatings sprayed on steel substrates.

Looking in more detail at the crystallinity index for the powder-sprayed coatings on Al substrates presented in Table 3 and on steel substrates presented in Table 4, it is apparent that the increase in the total gas flow rate from 2292 L/h (P1) to 2668 L/h (P3) up to 3000 L/h (P4) presents a minimum index (0.15 for the Al substrates and 0.20

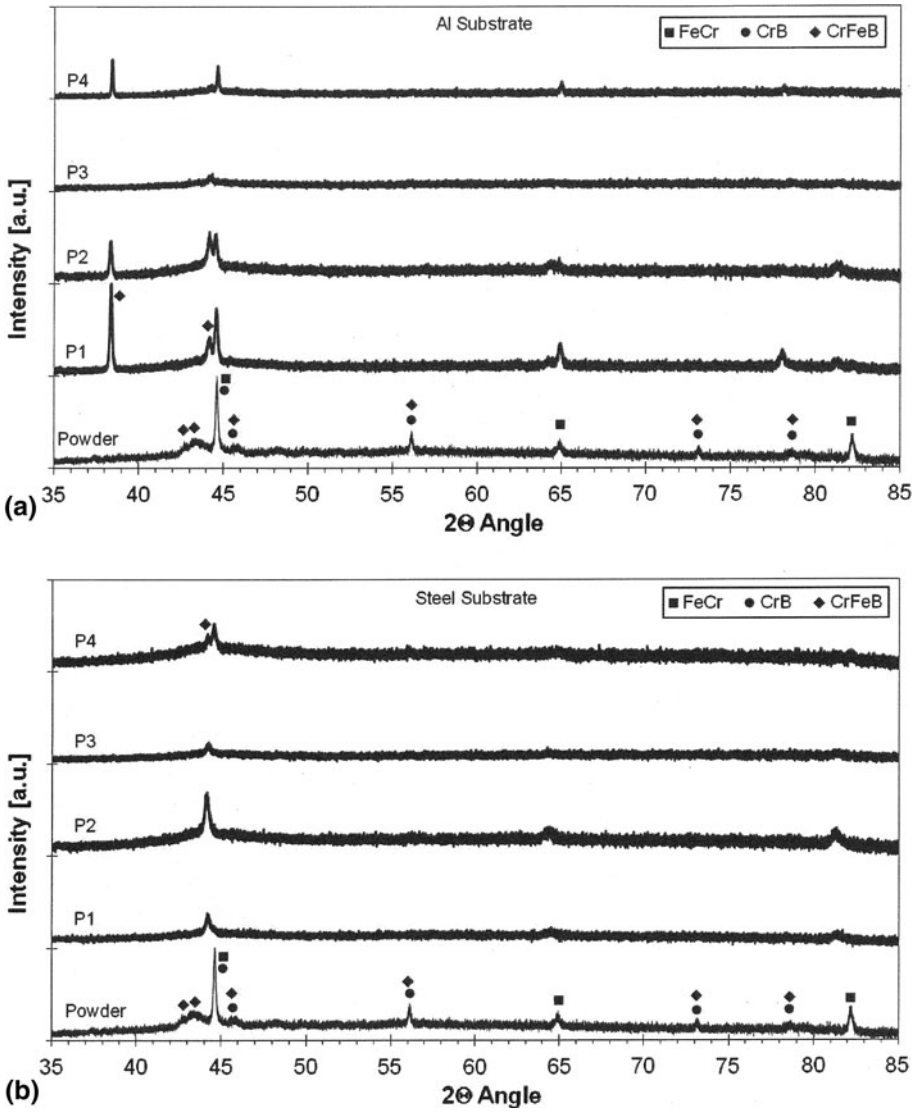

Fig. 3 XRD scans of the powder flame as-sprayed Fe-based coatings on (a) Al substrates and (b) steel substrates

for the steel substrates) obtained for the middle total gas flow rate of 2668 L/h (P3). The lower crystalline index of coating P3 may be explained by the higher velocity (due to the higher gas flow rate) and smaller diameter of the impinging particles, resulting in thinner splats and therefore shorter cooling times. For the coating P4, for which the total gas flow rate was the highest, it seems that the heat transfer may play a more significant role than the particle speed in the coating formation and its phase content than for the coating P3. Further experiments are necessary to fully understand the effect of the gas flow rate on the crystalline content of the as-sprayed coatings.

For the influence of the location of the cooling system on the crystallinity index during the powder spraying of the coatings (cooling system fixed (P1) or placed on the robot arm (P2)), it is seen that when using Al substrates, a decrease by a factor of 2 is observed when the cooling equipment moves with the robot. This can be explained by the fact that the displacement of the cooling system along with the robot acts like a quenching of the coatings during the spray process, which induces cooling times of the impinging splats shorter than when the cooling system is fixed in the spray booth. However, for the steel substrates, an increase in the index value by a factor of 2 occurs when the cooling system is placed on the robot arm. These discrepancies in the phase content of the coatings sprayed with or without a moving cooling system on either Al or steel substrates cannot be explained at this time and require further investigation.

A more detailed observation of the crystallinity indexes presented in Table 3 and 4 shows that for the powder-sprayed coatings on aluminum and steel substrates, the coatings with a high amorphization degree (i.e., a low crystallinity index) possess the highest hardness values. This is logical with the fact that an amorphous material should normally possess a higher hardness than its

crystalline counterpart. This influence of the crystallinity index on the hardness values of the sprayed coatings needs further detailed investigation.

3.3.2 Wire-Sprayed Coatings. Figure 4 shows the XRD patterns of the wire-sprayed coatings on both aluminum and steel substrates. The XRD pattern of the starting wire is also shown for comparison purposes.

In the feedstock wire, fewer phases were present than in the feedstock powder: only three peaks were detected and attributed to FeCr and CrB phases as the major phases. For the powder, the phases present in the wire as-sprayed coatings depend on the spray parameters used: for some coatings, new peaks are observed in addition to those already present in the feedstock powder; for other coatings, almost no peaks could be observed. The phases observed for the wire-sprayed coatings are similar to the reported elsewhere (Ref 5, 10, 11).

More precisely, for the coatings sprayed onto Al substrates, the sample W3 has a new CrFeB peak at an angle of 38° while maintaining the other main phases' starting wire peaks. However, for samples W4, no new peaks were observed and only a peak (44.5°) was detected with other small peaks. For samples W1 and W2, only an extremely weak peak (44.5°) was observed without any other peaks, which indicates that these coatings may be mostly amorphous.

For the coatings sprayed onto steel substrates, no samples show new peaks. Sample W4 has the strongest peak (44.5°) with other very small peaks, while samples W1, W2, and W3 have only an extremely weak peak at 44.5° with no other peaks, with sample W1 having the strongest peak of the three and sample W2 the weakest. Again, this indicates that the W1, W2, and W3 coatings may be predominantly amorphous.

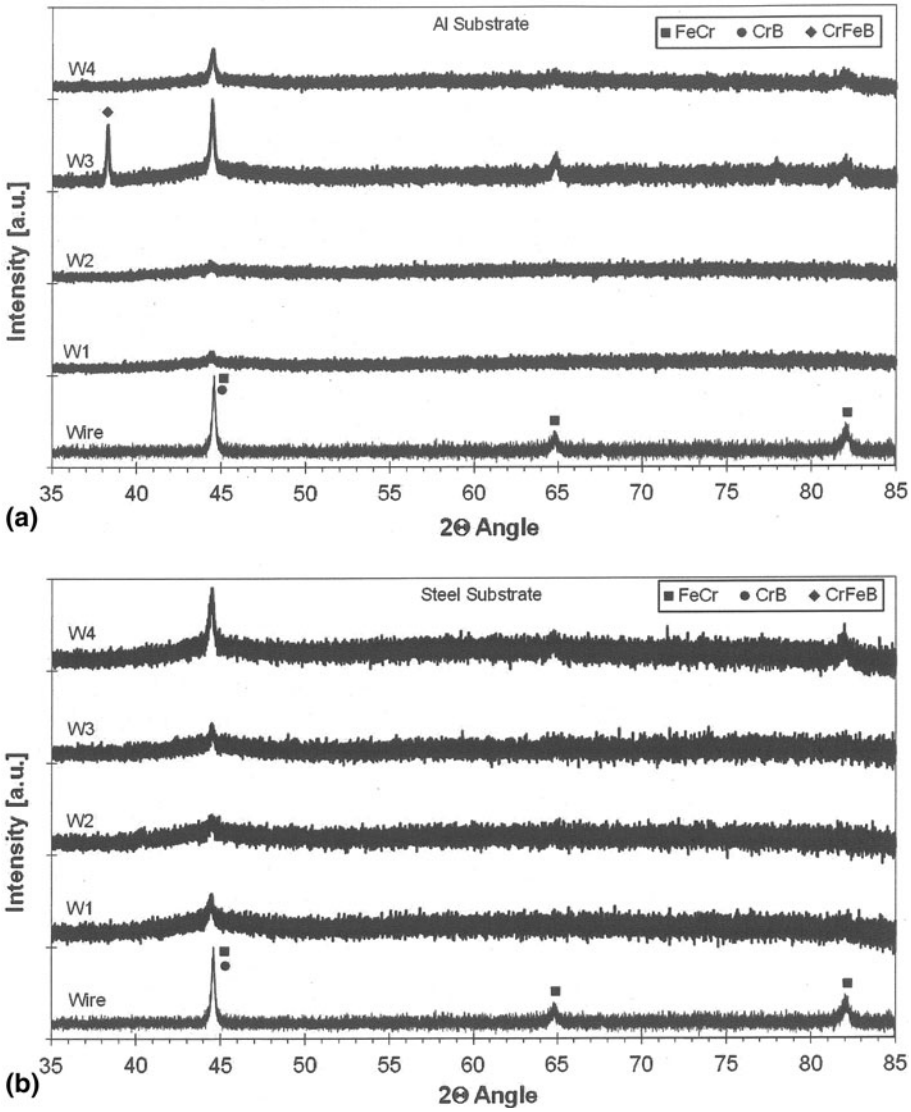

Fig. 4 XRD scans of the wire flame as-sprayed Fe-based coatings on (a) Al substrates and (b) steel substrates

When looking at the influence of the substrates on the phase content of the wire-sprayed coatings, the different phase contents of the coatings between the aluminum and steel substrates when using the same spray parameters are due, like for the powder-sprayed coatings presented previously, to the different heat conductivity of both substrates and therefore to the heat transfer occurring between the molten particles upon their impact with the substrates. Since heat transfer has a significant influence on the coating formation and phase content, the retention of the amorphous phase due to a very high cooling rate of the impinging molten spray particles is greatly influenced by the substrate material used.

Like the powder-sprayed coatings, the relative proportions of crystalline and amorphous or nanocrystalline phases were estimated by calculating the crystallinity index for all the wire-sprayed coatings on both substrate types (Al or steel). Table 3 lists the crystallinity index for the coatings sprayed on Al substrates and Table 4 for the coatings sprayed on steel substrates.

For the wire-sprayed coatings on Al substrates (Table 3), one can see that the crystallinity index decreases significantly from 0.97 to a value of 0.22 when the O_2/C_2H_2 ratio is increased from 1.0 (W3) to 1.6 (W1) and stays unchanged to 0.23 when the ratio is increased further to 2.0 (W2). For the steel substrates (Table 4), the index stays approximately unchanged when the O_2/C_2H_2 ratio is increased from 1.0 (W3: $I_c = 0.25$) to 1.6 (W1: $I_c = 0.31$) and further to 2.0 (W2: $I_c = 0.24$).

For the influence of the total gas flow rate on the crystallinity index during the wire spraying of the coatings, it is observed that independent of the substrate used, the index increases significantly (by a factor slightly higher than 2 for the Al substrates and by 50% for the steel substrates) when the flow rate is increased from 2292 L/h (W1) to 3000 L/h (W4). This increase in the crystalline index when the gas flow rate is increased could not be explained by assuming that a higher velocity of the impinging particles results in thinner splats and shorter cooling times, producing more amorphous coatings as described earlier for the powder-sprayed coatings. It is thus expected that in the wire-spraying process, the higher gas flow rate may produce larger molten wire droplets which result in bigger splats and longer cooling times, long enough to enable the crystallization of the sprayed coatings.

Again, as for the powder-sprayed coatings, a more detailed observation of the crystallinity indexes presented in Table 3 and 4 shows that for the wire-sprayed coatings on steel substrates, the coatings with a high degree of amorphization possess the highest hardness values. On the other hand, for the wire-sprayed coatings on aluminium substrates, the inverse is observed, i.e., the coatings with a low amorphization level possess the highest hardness, which is not logical since an amorphous material normally possess a higher hardness than its crystalline counterpart. This influence of the crystallinity index on the hardness values of the sprayed coatings needs further detailed investigation.

3.4 Wear Resistance

Figure 5 shows the wear rate of the powder and wire as-sprayed Nanosteel coatings on both aluminum and steel substrates. Independent of the feedstock type (powder or wire) and the substrate used (Al or steel), the applied coatings possess a greatly reduced wear rate in comparison with the uncoated substrates. The coatings P3 and W3 show the lowest wear rate for both the aluminum- and steel-sprayed substrates. The P3 coating has the highest hardness and the lowest crystallinity index on both the Al and steel substrates, i.e., the coating with the highest amorphous proportion. The W3 coating has the highest hardness on both the Al and steel substrates and one of

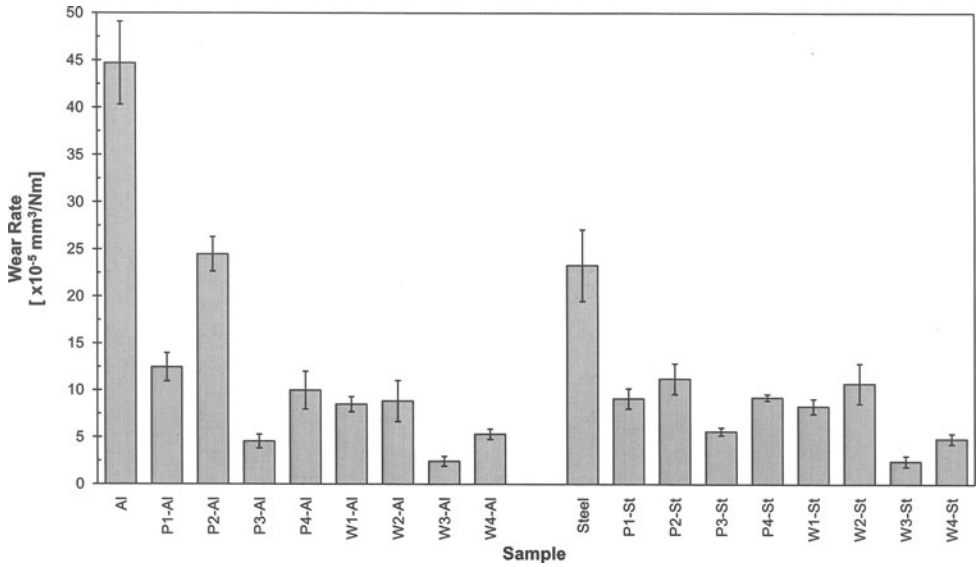

Fig. 5 Wear rate of the powder (P) and wire (W) as-sprayed Fe-based coatings on Al and steel substrates

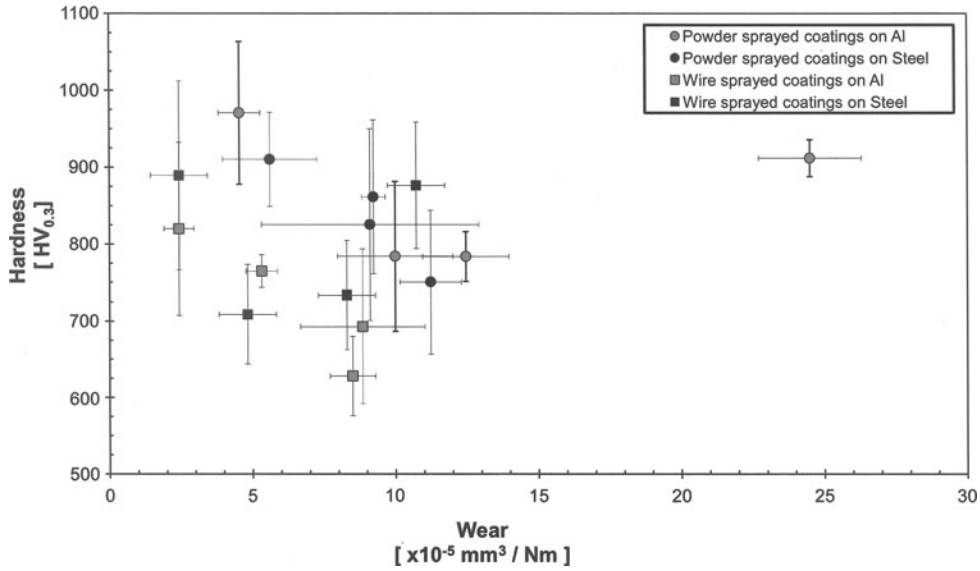

Fig. 6 Hardness as a function of the wear rate of the powder and wire as-sprayed Fe-based coatings on Al and steel substrates

the lowest crystallinity indexes on the steel substrate, but on the Al substrate its crystallinity index is the highest. Further investigations are underway to clarify the reasons for the excellent wear behavior of this crystalline coating in comparison with the other more amorphous coatings.

A significant direct comparison of the wear resistance results obtained in this study with results published elsewhere is not straightforward, because, firstly, the wear resistance of such thermally sprayed iron-based amorphous coatings has not been thoroughly investigated, and secondly, the reported wear tests differ somewhat from the present ball-on-disk test. However, an approximate comparison of the wear resistance can be performed with the wear results of HVOF-sprayed iron-based amorphous coatings published by Branagan et al. (Ref 4), in which the ASTM-G65 Procedure A wear test was applied with a load of 130 N and duration of 6000 cycles, which represented a linear distance of 4309 m. The wear volume loss of such coatings in the as-sprayed condition was approximately 45 mm^3, which represents a wear rate of approximately 8×10^{-5} mm^3/N m, which is about a factor of 2 higher than the best powder- or wire flame-sprayed iron-based amorphous coatings presented in this study. Since the comparison of the wear test results took place between two different tests, to stay on the safe side one may say that the flame-spray process (either with powder or wire as the raw material) can produce iron-based amorphous coatings with a wear resistance similar to the same coatings produced using much more expensive thermal spray processes such as HVOF. Therefore, the flame-spray process may represent a cost-effective alternative in the production of highly wear-resistant iron-based amorphous coatings.

An inverse relation between hardness and wear volume loss is general in most materials. Except for two samples (P2 on Al and W2 on steel), this relation was also found in this study, as shown in Fig. 6. Both coatings, P2 on Al and W2 on steel, possess hardness values similar to those of other coatings (such as P3 on Al and W3 on steel) but have a much higher wear volume loss, which excludes this inverse relation between hardness and wear rate. Since their porosity level is similar to the other coatings, this indicates that the microstructure of these coatings has a more important influence on their wear behavior than their porosity level.

4. Conclusions

The powder flame-spraying process represents an efficient alternative to other thermal spray techniques due to its low equipment costs, lower gas consumption, and ease of application for producing amorphous iron-based coatings intended for wear applications. The coatings it produces possess microstructures which are of slightly less quality and which have slightly lower hardness values, but their wear resistance is similar to that of coatings produced using plasma or HVOF-spray techniques. Thus, the properties of flame-sprayed coatings suffice for use in protecting the surfaces of aluminum alloys or steel parts. In addition, the flame-spray process is easier to use on-site and is also better suited to coating small parts due to the lower heating of the substrate and the lower quantity of overspray.

The hardness of flame-sprayed coatings depends on the spray parameters used and is slightly lower than that of plasma- or HVOF-sprayed coatings. This is believed to be due to the lower impact velocity combined with the lower particle temperature encountered in the flame-spray process.

Flame-spray coating wear resistance is also strongly dependent on the parameters used. However, iron-based flame-sprayed coatings possess a wear resistance similar to that of coatings produced using plasma or HVOF processes.

In conclusion, this study demonstrates that powder and wire flame spraying of amorphous iron-based coatings represents a viable alternative to plasma and HVOF spray techniques for producing wear-resistant coatings. However, further investigations are needed to optimize the coating microstructures to improve wear resistance and to fully understand the influence of spray parameters on coating properties.

Acknowledgments

The author is grateful to Christa Kainhofer for her technical support in metallographic preparation and microscopy analysis of sample microstructures; Andreas Schiffl for performing the porosity measurements; Prof. Dr. Peter J. Uggowitzer and Petra Gunde for performing the X-Ray diffraction analysis; and Thomas Müller from Rübig for the leasing of the tribometer used to perform wear tests.

References

1. B.B. Kappes, B.E. Meacham, Y.L. Tang, and D.J. Branagan, Relaxation, Recovery, Crystallization, and Re-Crystallization Transformations in an Iron-Based Amorphous Precursor, *Nanotechnology*, 2003, **14**, p 1228-1234
2. D.J. Branagan, M.C. Marshall, and B.E. Meacham, Formation of Nanoscale Composite Coatings via HVOF and Wire-Arc Spraying, *Proceedings of the International Thermal Spray Conference 2005*, May 2-4, 2005 (Basel, Switzerland), on CD-ROM
3. P. Georgieva, R. Thorpe, A. Yanski, and S. Seal, A Novel Nano-Composite Wire Material: The Low Cost and Enhanced Properties Coating Design, *Proceedings of the International Thermal Spray Conference 2006*, May 15-18, 2006 (Seattle, WA), on CD-ROM
4. D.J. Branagan, M.C. Marshall, B.E. Meacham, L.F. Aprigliano, R. Bayles, E.J. Lemieux, T. Newbauer, F.J. Martin, J.C. Farmer, J.J. Haslam, and S.D. Day, Wear and Corrosion Resistant Amorphous/Nanostructured Steel Coatings for Replacement of Electrolytic Hard Chromium, *Proceedings of the International Thermal Spray Conference 2006*, May 15-18, 2006 (Seattle, WA), on CD-ROM
5. P. Rohan, S. Bouaricha, J.G. Legoux, C. Moreau, A. Denoirjean, A. Vardelle, and C. Le Niniven, Deposition and Crystallization of Thermally Sprayed Amorphous Metallic Coatings, *Proceedings of the International Thermal Spray Conference 2005*, May 2-4, 2005 (Basel, Switzerland), on CD-ROM
6. Y. Wu, P. Lin, G. Xie, J. Hu, and M. Cao, Formation of Amorphous and Nanocrystalline Phases in High Velocity Oxy-Fuel Thermally Sprayed a Fe-Cr-Si-B-Mn Alloy, *Mater. Sci. Eng. A*, 2006, **430**, p 34-39
7. M. Parco, I. Fagoaga, K. Bobzin, E. Lugscheider, J. Zwick, and G. Hidalgo, Development and Characterization of Nanostructured Iron-Based Coatings by HFPD and HVOF, *Proceedings of the International Thermal Spray Conference 2006*, May 15-18, 2006 (Seattle, WA), on CD-ROM
8. K. Bobzin, E. Lugscheider, F. Ernst, J. Zwick, T. Schlaefer, C. Verpoort, A. Schwenk, F. Schreiber, T. Wenz, D. Cook, K. Kowalsky, and J. Conti, Coating Bores of Light Metal Crankcases, *Proceedings of the International Thermal Spray Conference 2006*, May 15-18, 2006 (Seattle, WA), on CD-ROM
9. D.J. Branagan, M. Breitsameter, B.E. Meacham, and V. Belashchenko, High-Performance Nanoscale Composite Coatings for Boiler Applications, *J. Thermal Spray Technol.*, 2005, **14**(2), p 196-204
10. H.W. Jin, C.G. Park, and M.C. Kim, Microstructure and Amorphization Induced by Frictional Work in Fe-Cr-B Alloy Thermal Spray Coatings, *Surf. Coat. Technol.*, 1999, **113**, p 103-112
11. D. Shin, F. Gitzhofer, and C. Moreau, Development of Metal Based Thermal barrier Coatings (MBTBCs) for Low Heat Rejection Diesel Engines, *Proceedings of the International Thermal Spray Conference 2005*, May 2-4, 2005 (Basel, Switzerland), on CD-ROM